JACS
JOURNAL OF THE AMERICAN CHEMICAL SOCIETY
Communication
pubs.acs.org/JACS

Curvature Softening and Negative Compressibility of Gel-Phase Lipid Membranes

Patrick Diggins IV, Zachary A. McDargh, and Markus Deserno*

Department of Physics, Carnegie Mellon University, Pittsburgh, Pennsylvania 15213, United States

Supporting Information

ABSTRACT: We show that gel-phase lipid membranes soften upon bending, leading to curvature localization and a negative compressibility. Using simulations of two very different lipid models to quantify shape and stress−strain relation of buckled membranes, we demonstrate that gel phase bilayers do not behave like Euler elastica and hence are not well described by a quadratic Helfrich Hamiltonian, much unlike their fluid-phase counterparts. We propose a theoretical framework which accounts for the observed softening through an energy density that smoothly crosses over from a quadratic to a linear curvature dependence beyond a critical new scale l^{-1}. This model captures both the shape and the stress−strain relation for our two sets of simulations and permits the extraction of bending moduli, which are found to be about an order of magnitude larger than the corresponding fluid phase values. We also find surprisingly large crossover lengths l, several times bigger than the bilayer thickness, rendering the exotic elasticity of gel-phase membranes more strongly pronounced than that of homogeneous compressible sheets and artificial metamaterials. We suggest that such membranes have unexpected potential as nanoscale systems with striking materials characteristics.

Much effort has recently gone into synthesis and characterization of novel materials with exotic properties, pertaining for instance to their chemistry, optics, and mechanics.[1−4] The latter in particular plays a dual role as both a primary function and a secondary constraint on design, processing, and structural integrity. Since elasticity reveals its unique characteristics beyond linear response, much work has focused on stability limits and large deformations, and for both subjects buckling is the most widely studied example.[5−12] For instance, several systems have been shown to exhibit curvature localization and negative compressibility, properties that may exacerbate a material's failure modes, but which, if properly utilized, enable novel applications in mechanical sensors and microactuators.[8−12] These phenomena have been observed under a variety of circumstances, ranging from wide isotropic beams[12] to floating elastica[10,11] to metamaterials,[12] but how the underlying microscopic characteristics lead to dramatic large-scale properties remains puzzling. A better understanding of this connection would permit exciting advances in rational materials design and chemistry.

Here we demonstrate that lipid membranes in the gel phase buckle discontinuously, as curvature softening leads to a negative compressibility. The effect is more pronounced compared to unstructured sheets and manifests at the nanoscale, far smaller than for other materials. This phenomenon is very surprising, given that fluid-phase membranes follow classical curvature elasticity and buckle exactly like Euler elastica,[13,14] as we also confirm in more detail. Since the exotic behavior can be triggered by cooling below the main phase transition, which in turn can be tuned over a wide range by using suitable lipids or mixtures, lipid membranes emerge as attractive model systems for exotic elasticity and promising material candidates for switchable elastic nano devices, especially given the vast information already available concerning their structure and thermodynamics.

Before we discuss gel membrane elasticity, let us recall the canonical starting point for fluid membrane elasticity: the Helfrich Hamiltonian.[15] It models a membrane as a two-dimensional surface equipped with the curvature energy density:

$$e(K, K_G) = \frac{1}{2}\kappa(K - K_0)^2 + \bar{\kappa}K_G \tag{1}$$

where K and K_G are total and Gaussian surface curvature, respectively.[16,17] The mean and Gaussian curvature moduli, κ and $\bar{\kappa}$, as well as the spontaneous curvature K_0 need to be either calculated from more finely resolved theories or determined in experiment or simulation. "Measuring the bending rigidity of gel-phase membranes" presumes that such low-temperature bilayer phases also follow a Hamiltonian of the form (eq 1), just with different values for the moduli. We will show that this assumption is critically incomplete, with significant quantitative implications for the inferred material parameters.

The many simulation techniques for determining the rigidity κ of fluid bilayers essentially divide into two classes: monitoring passive fluctuations[18−32] and imposing active deformations.[13,14,33,34] The former exploit the fact that suitably chosen fluctuation modes are inversely proportional to κ, while the latter measure the force needed to bend a membrane, which is directly proportional to κ. The passive methods are currently more widely used, but the inverse relation between rigidity and fluctuations causes difficulties when working with gel phases: their moduli are believed to exceed those of fluid bilayers by about an order of magnitude,[35−37] and hence the observed signal (a fluctuation) is a lot harder to detect. In contrast, for active methods the signal (a force) increases by that same factor. Measuring the elastic response to active deformations appears to be the more promising route for gel phases.

Before specifically discussing gel phases, let us briefly review the main idea of buckling, as previously applied to the fluid case.[13,14]

Received: June 30, 2015
Published: September 28, 2015

DOI: 10.1021/jacs.5b06800
J. Am. Chem. Soc. 2015, 137, 12752−12755

Table 1. Properties of the Two Lipid Models

property	Cooke	MARTINI
lipid	$w_c/\sigma = 1.6$[a]	DMPC[b]
beads/lipid	3	10
solvent	none	1 bead = 4 H_2O
N_{lipids}	1344	1170
P_2(gel) /P_2(fluid)	0.957/0.732	0.858/0.369
T	$0.85\varepsilon/k_B$[a]	265 K
L	54.2σ	432 Å
L_y	12.0σ	61.3 Å

[a]σ and ε are Lennard-Jones units. For the Cooke model, a good approximate mapping of length is $\sigma \approx 11$ Å. [b]DMPC = 1,2-dimyristoyl-*sn*-glycero-3-phosphocholine, or (14:0)-PC.

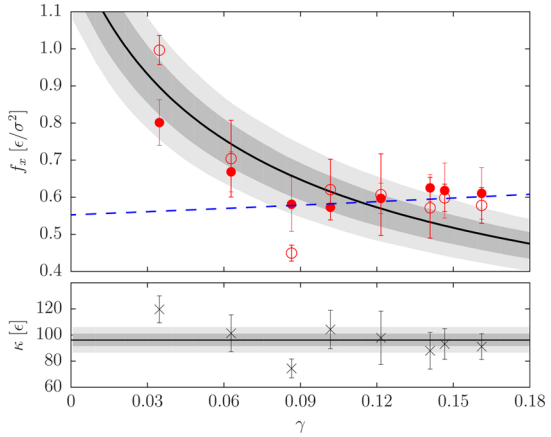

Figure 1. Top: Buckling stress f_x as a function of strain γ for the Cooke model. The open circles are calculated directly from the stress tensor. The filled circles are calculated by scaling $\tilde{f}_x$ with κ/l^2, where $\tilde{f}_x$ and l are inferred from the shapes of each simulation and κ is taken from the measured stresses by averaging over all simulations. The blue dashed line is the poor fit to the Euler stress; the solid curve is our new prediction for $f_x(\gamma)$, determined from the average value of $\tilde{f}_x$ and l. Its flanking 68% and 95% confidence bands are based on resampling all data. Bottom: bending rigidity κ derived from each simulation.

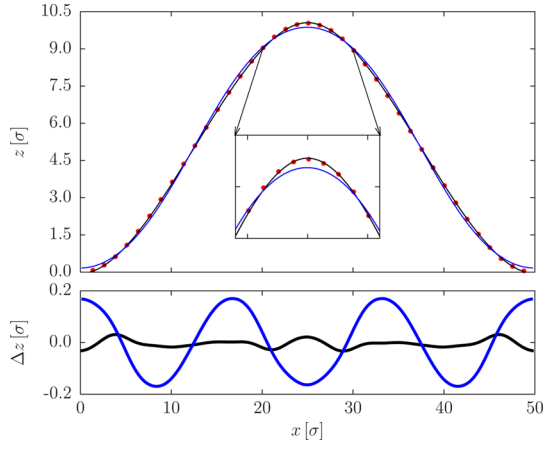

Figure 2. Comparison between simulated and calculated gel buckle shape. Top: average shape of a Cooke model buckle at $\gamma = 7.7\%$ (red circles); the vertical axis is stretched approximately 3-fold for better visibility. The blue line is the predicted Euler buckle shape, the black line is the best fit based on the energy density (3a), using l as the fitting parameter. Bottom: residuals between simulation and the two theories (same coloring as top). The rmsd from eq (S15) in the SI for the Euler buckle is 0.122σ, our extended theory gives 0.015σ, nearly an order of magnitude smaller.

An incompressible membrane buckles if it is forced into a box of cross-sectional area smaller than the equilibrium area of the membrane. By choosing a strongly elongated rectangle as that area, a single buckle develops along the extended direction, say the x-axis. The buckle's overall bending energy is the area integral of the energy density (eq 1), which is minimized by a shape belonging to the class of planar Euler elastica.[38] It can be expressed analytically in terms of Jacobi elliptic functions and integrals.[38,39] This equilibrium shape depends only on the size of the membrane, not on its rigidity, and hence comparing the predicted shape with the observed one permits a parameter-free test of the theory. One can further calculate the stress (or force per unit length) f_x required to achieve a buckling strain $\gamma = (L - L_x)/L$, where L_x is the box-length along the buckle's undulation direction and L is the total contour length of the membrane along the buckle:[14]

$$f_x(\gamma) = \kappa\left(\frac{2\pi}{L}\right)^2\left[1 + \frac{1}{2}\gamma + \frac{9}{32}\gamma^2 + \frac{21}{128}\gamma^3 + \cdots\right] \quad (2)$$

This stress contains κ as the only fitting parameter and therefore provides easy access to the mean curvature modulus.

We can apply the buckling method, as described so far, also to gel-phase membranes, because the shape change is isometric, and so the Gaussian curvature remains zero. We will use two different lipid models: Cooke[40,41] and MARTINI.[42] The Cooke model is a low-resolution coarse-grained implicit solvent model where each lipid is represented by three particles; MARTINI is a highly versatile medium-resolution explicit solvent coarse-grained model, and we chose DMPC (10 particles) as the lipid. Both models are well discussed in the literature, and we will leave further details to the Supporting Information (SI). With this choice we cover two different resolutions and both explicit and implicit solvents. We deliberately forego atomistic modeling, since the (substantial) equilibration issues are not our main focus; however, we wish to stress that buckling is a viable protocol even for high-resolution explicit-solvent models, as we have demonstrated for the fluid case.[14] For the Cooke simulations, we used the ESPResSo package,[43] and for the MARTINI simulations, we used GROMACS 4.5.[44] The Python toolkit MDAnalysis[45] was also used for further analysis. More details, including a discussion on the difficulty to equilibrate gel-phase membranes, can be found in the SI.

Figure 1 shows the stress–strain relation for the Cooke model resulting from such a set of simulations. It is clear that the results do not match the prediction from eq 2 based on Helfrich theory, not even qualitatively: the stress decreases as strain increases, implying a negative compressibility. And if we naïvely fit the data, we obtain an unrealistically small value of κ, only about three times larger than in the fluid case. Hence, Helfrich theory appears not to properly describe gel-phase membranes.

To trace down the origin of this discrepancy, we compare the shape of the gel buckles to the prediction from Helfrich theory. We project the particles closest to the pivotal plane of each monolayer to the bilayer's midplane and expand the result in a Fourier series (see SI). For a Cooke buckle at $\gamma = 7.7\%$, Figure 2 compares the classical Euler shape (blue curve) with the observed one (red circles). Again, theory disagrees with simulation: curved regions at the turning points are more curved than the Euler prediction, while flat regions are flatter. The deviation appears small, but it is systematic and does not occur for fluid buckles (see SI). It has profound consequences, as we will now discuss.

The curvature localization revealed by our shape analysis suggests that the energy penalty for high bending is lower than

DOI: 10.1021/jacs.5b06800
J. Am. Chem. Soc. 2015, 137, 12752–12755

what eq 1 assumes. An obvious way for capturing this effect is to extend Helfrich theory by a quartic term. Softening at larger curvatures means it must have a negative prefactor, but this would result in an energy density that is not bounded below. We need to regularize such a theory by adding even higher order terms, ideally without introducing more arbitrary parameters. We propose to use a functional form that crosses over from a quadratic to a linear dependence at some curvature scale l^{-1}, thus staying both bounded below and convex:

$$\tilde{e}(K) = \kappa l^{-2}[\sqrt{1 + l^2K^2} - 1] \tag{3a}$$

$$= \begin{cases} \frac{1}{2}\kappa K^2 - \frac{1}{8}(\kappa l^2)K^4 + O(K^6), & K \ll l^{-1} \\ \kappa l^{-1}(|K| - l^{-1}) + O(K^{-1}), & K \gg l^{-1} \end{cases} \tag{3b}$$

This effectively amounts to a specific choice for regularization. Since for sufficiently small curvature postquartic terms will matter little, all we require is that they introduce neither unnecessary structure nor undue mathematical complication, and both holds for our choice. For example, some empirical suggestions for capturing curvature softening let $e(K)$ cross over into a plateau (instead of growing further, even though only linearly); this will by construction permit kinking once the curvature exceeds some critical threshold.[46,47]

We dropped the Gaussian term $\bar{\kappa}K_G$ in our extended theory (eq 3a), because we strive to understand planar buckles, for which $K_G = 0$, and so we can ignore it, along with two other possible quartic terms, namely K^2K_G and $K_G{}^2$. However, there exists yet another term, the curvature gradient $(\nabla K)^2$, which does not vanish for buckles and is also of order length^{-4}. Softening would again correspond to a negative prefactor, but this time regularization can not be achieved as easily as in the K^4 case. Moreover, this gradient term would increase the order of the resulting Euler−Lagrange differential equation by 2, rendering the mathematics substantially more onerous. While neither of these troubles imply that such a term does not exist, we will see that it is not needed to obtain satisfactory agreement between simulation and theory. We will therefore ignore the gradient term, if only for pragmatic reasons.

To predict a buckle's shape we need to solve the Euler−Lagrange equation corresponding to the functional (eq 3a). We describe the shape through the angle $\psi(s)$ of the profile's tangent vector $\vec{t}$ with respect to the horizontal as a function of arclength s, such that $K = -\psi' \equiv -\mathrm{d}\psi/\mathrm{d}s$.[13,14] Stress conservation along the x-axis again leads to a first integral.[14,48] Choosing the origin of s such that $\psi(0) = \psi_i$, the remaining quadrature takes the form:

$$\frac{s}{l} = \int_{\psi_i}^{\psi(s)} \mathrm{d}\psi\{[1 - \tilde{f}_x(\cos\psi - \cos\psi_i)]^{-2} - 1\}^{-1/2} \tag{4}$$

where the parameter $\tilde{f}_x = f_x l^2/\kappa \equiv l^2/\lambda^2$ is a dimensionless measure of the stress confining the buckle. The spatial coordinates can be determined by integrating the components of the tangent vector $\vec{t} = (x'(s), y'(s)) = (\cos\psi, \sin\psi)$.

The same series-inversion techniques we used for the fluid case[14] lead to the stress−strain relation, valid for small strain. Defining the dimensionless parameter $\delta = 2\pi l/L$, we obtain

$$f_x(\gamma, \delta) = \kappa\left(\frac{2\pi}{L}\right)^2\left[1 + \frac{1}{2}(1 - 3\delta^2)\gamma + O(\gamma^2)\right] \tag{5}$$

which reduces to eq 2 in the limit $\delta \to 0$. Unfortunately, once we have $\delta^2 > 1/3$, this series no longer converges for all γ, but in that case we can still integrate the quadrature numerically.

Table 2. Moduli, Crossover Length, And Bilayer Width for Our Simulations

model	κ_{fl} $[k_BT_{fl}]^{a,b}$	κ_{gel} $[k_BT_{gel}]^{b}$	l (Å)	w (Å)^{c}
Cooke	12.8(4)	96(5)	275(22)	52.9
MARTINI	29(1)	230(10)	139(5)	39.0

[a]Values from Hu et al.[14] [b]Temperature differs between fluid and gel phase: for the Cooke model, $T_{fl} = 1.1\ \varepsilon/k_B$ for the fluid and $T_{gel} = 0.85\ \varepsilon/k_B$ for the gel phase. For MARTINI DMPC, $T_{fl} = 300$ K and $T_{gel} = 265$ K. [c]Bilayer width w is measured as the distance between head beads and phosphate beads in opposing planes for Cooke and MARTINI, respectively.

How well does our modified theory describe the gel-phase simulations? We begin with the shape comparison. The black line in Figure 2 shows that the extended theory (eq 3a) captures the simulated shape much more accurately than the Euler buckle did. We can quantify this by the shape's root-mean-square deviation (rmsd). For instance, the Euler buckle in Figure 2 gives an rmsd of 0.122 σ, while the rmsd drops by almost an order of magnitude to 0.015 σ for our extended theory (eq 3a). This is also visually illustrated by the residuals in the bottom part of Figure 2.

Next, the black curve in Figure 1 shows the prediction for the stress−strain relation, $f_x(\gamma, \langle\delta\rangle)$, taking the average value for l (and hence $\langle\delta\rangle = 2\pi\langle l\rangle/L$) extracted from all shapes and using the best fit for κ over the entire set of data. Unlike eq 2, our new theory captures the observed negative compressibility; this equally holds for the MARTINI simulations, as documented in the SI. Eq 5 predicts that the compressibility will turn negative once $\delta > 1/\sqrt{3} \approx 0.58$. We find $\delta = 2.9$ and 2.0 for Cooke and MARTINI, respectively, far beyond critical.

The material parameters derived from our fits are summarized in Table 2. For both models κ/k_BT is almost an order of magnitude larger in the gel phase than in the fluid phase, in better agreement with expectation.[35−37] The seemingly minor shape deviation between the gel-phase simulation and the Euler buckle prediction profoundly affects the inferred moduli. Moreover, in both cases the deduced crossover length l is significantly larger than the bilayer thickness w, explaining why the higher order correction is noticeable even at very weak buckling. For instance, the buckle at $\gamma = 7.7\%$ in Figure 2 has a smallest curvature radius of $R \approx 0.28L \approx 167$ Å $\approx 0.6\,l$. Notice finally that the two models have different crossover lengths l, with the value for the Cooke model being about twice that of MARTINI DMPC. This is not surprising, given how different the models are, but it shows that the extent to which deviations from Helfrich elasticity occur will depend on the model, and surely also on the lipid.

Oshri and Diamant have recently shown that our extended curvature functional (eq 3a) arises naturally when describing homogeneous thin compressible elastics.[49] Their framework (combined with thin plate theory[48,50]) predicts that the crossover length is very small, $l = w/\sqrt{48}$, implying that a negative compressibility only occurs for unrealistic width-to-length ratios $w/L > 2/\pi \approx 64\%$, for which thin-plate theory is of course no longer valid. Accounting for finite-width corrections, Coulais et al. show, using both experiments and numerics, that this critical ratio drops to 12%;[12] in experiments with internally patterned metamaterial beams they can get as low as 5%.[12] Compared to this, our Cooke and MARTINI models exhibit the even smaller critical aspect ratios of 1.8% and 2.6%, a more striking elastic response than artificially designed metamaterials. This suggests that real gel-phase membranes are promising candidates for exotic elastic properties. Given that a membrane's main phase transition is easily

DOI: 10.1021/jacs.5b06800
J. Am. Chem. Soc. 2015, 137, 12752−12755

tunable by lipid type and composition and that we have decades worth of experimental, computational, and theoretical insight into these systems, gel phases are nearly ideal model systems and test beds for probing, understanding, and applying exotic elasticity.

It is remarkable that the membranes we simulated, which were neither small nor exceptionally strongly bent, are well past the discontinuous buckling threshold. We therefore expect most simulations of curved gel phases to experience curvature softening, and so analyzing them on the quadratic level may be insufficient. What is more, the discovery of K^4 corrections feeds the suspicion that the other quartic terms, K^2K_G, $K_G{}^2$, and $(\nabla K)^2$, come with moduli of comparable magnitude, but our buckling protocol is insensitive to the first two and cannot easily disentangle the third gradient term from the K^4 term. Hence, we likely have no accurate elastic theory to describe prominent applications of gel-phase membranes, e.g., their use as temperature-sensitive liposomal drug carriers.[51−53] Developing such a theory will be a necessary step toward exploiting the potential of these phases more systematically. For instance, understanding the role of a bilayer's microstructure (such as order parameter, tilt, and prestress) would help to predict how analogous but artificial materials (such as diblock copolymer membranes) need to be designed to mimic or even amplify such exotic elastic behavior.

■ ASSOCIATED CONTENT

Supporting Information

The Supporting Information is available free of charge on the ACS Publications website at DOI: 10.1021/jacs.5b06800.

Details of the simulation setup as well as additional figures and theoretical arguments (PDF)

■ AUTHOR INFORMATION

Corresponding Author

*deserno@andrew.cmu.edu

Notes

The authors declare no competing financial interest.

■ ACKNOWLEDGMENTS

We thank Haim Diamant and Oz Oshri for stimulating discussions. Support from NSF grant CHE-1464926 is also gratefully acknowledged.

■ REFERENCES

(1) Yu, C. H.; Schubert, C. P.; Welch, C.; Tang, B. J.; Tamba, M.-G.; Mehl, G. H. *J. Am. Chem. Soc.* **2012**, *134*, 5076−5079.
(2) Ungur, L.; Langley, S. K.; Hooper, T. N.; Moubaraki, B.; Brechin, E. K.; Murray, K. S.; Chibotaru, L. F. *J. Am. Chem. Soc.* **2012**, *134*, 18554−18557.
(3) Xia, F.; Jiang, L. *Adv. Mater.* **2008**, *20*, 2842−2858.
(4) Shalaev, V. M. *Nat. Photonics* **2007**, *1*, 41−48.
(5) Isenberg, H.; Kjaer, K.; Rapaport, H. *J. Am. Chem. Soc.* **2006**, *128*, 12468−12472.
(6) Liu, D.; Peng, X.; Wu, B.; Zheng, X.; Chuong, T. T.; Li, J.; Sun, S.; Stucky, G. D. *J. Am. Chem. Soc.* **2015**, *137*, 9772−9775.
(7) Azuma, M.; Yoshida, H.; Saito, T.; Yamada, T.; Takano, M. *J. Am. Chem. Soc.* **2004**, *126*, 8244−8246.
(8) Pocivavsek, L.; Dellsy, R.; Kern, A.; Johnson, S.; Lin, B.; Lee, K. Y. C.; Cerda, E. *Science* **2008**, *320*, 912−916.
(9) Diamant, H.; Witten, T. A. *Phys. Rev. Lett.* **2011**, *107*, 164302.
(10) Diamant, H.; Witten, T. A. *Phys. Rev. E* **2013**, *88*, 012401.
(11) Oshri, O.; Brau, F.; Diamant, H. *Phys. Rev. E* **2015**, *91*, 052408.
(12) Coulais, C.; Overvelde, J. T. B.; Lubbers, L. A.; Bertoldi, K.; van Hecke, M. *Phys. Rev. Lett.* **2015**, *115*, 044301.
(13) Noguchi, H. *Phys. Rev. E* **2011**, *83*, 061919.
(14) Hu, M.; Diggins, P.; Deserno, M. *J. Chem. Phys.* **2013**, *138*, 214110.
(15) Helfrich, W. Z. *Naturforsch. C* **1973**, *28*, 693−703.
(16) Kreyszig, E. *Differential Geometry*; Dover: New York, 1991.
(17) do Carmo, M. *Differential Geometry of Curves and Surfaces*; Prentice Hall: Englewood Cliffs, NJ, 1976.
(18) Goetz, R.; Gompper, G.; Lipowsky, R. *Phys. Rev. Lett.* **1999**, *82*, 221−224.
(19) Lindahl, E.; Edholm, O. *Biophys. J.* **2000**, *79*, 426−433.
(20) Marrink, S. J.; Mark, A. E. *J. Phys. Chem. B* **2001**, *105*, 6122−6127.
(21) Ayton, G.; Voth, G. A. *Biophys. J.* **2002**, *83*, 3357−3370.
(22) Marrink, S. J.; de Vries, A. H.; Mark, A. E. *J. Phys. Chem. B* **2004**, *108*, 750−760.
(23) Brannigan, G.; Philips, P. F.; Brown, F. L. H. *Phys. Rev. E* **2005**, *72*, 011915.
(24) Wang, Z.-J.; Deserno, M. *J. Phys. Chem. B* **2010**, *114*, 11207−11220.
(25) Brandt, E. G.; Braun, A. R.; Sachs, J. N.; Nagle, J. F.; Edholm, O. *Biophys. J.* **2011**, *100*, 2104−2111.
(26) Shiba, H.; Noguchi, H. *Phys. Rev. E* **2011**, *84*, 031926.
(27) May, E. R.; Narang, A.; Kopelevich, D. I. *Phys. Rev. E* **2007**, *76*, 021913.
(28) Watson, M. C.; Brandt, E. G.; Welch, P. M.; Brown, F. L. H. *Phys. Rev. Lett.* **2012**, *109*, 028102.
(29) Watson, M. C.; Penev, E. S.; Welch, P. M.; Brown, F. L. H. *J. Chem. Phys.* **2011**, *135*, 244701.
(30) Johner, N.; Harries, D.; Khelashvili, G. *J. Phys. Chem. Lett.* **2014**, *5*, 4201−4206.
(31) Khelashvili, G.; Kollmitzer, B.; Heftberger, P.; Pabst, G.; Harries, D. *J. Chem. Theory Comput.* **2013**, *9*, 3866−3871.
(32) Levine, Z. A.; Venable, R. M.; Watson, M. C.; Lerner, M. G.; Shea, J.; Pastor, R. W.; Brown, F. L. H. *J. Am. Chem. Soc.* **2014**, *136*, 13582−13585.
(33) Harmandaris, V. A.; Deserno, M. *J. Chem. Phys.* **2006**, *125*, 204905.
(34) Arkhipov, A.; Yin, Y.; Schulten, K. *Biophys. J.* **2008**, *95*, 2806−2821.
(35) Lee, C.-H.; Lin, W.-C.; Wang, J. *Phys. Rev. E: Stat. Phys., Plasmas, Fluids, Relat. Interdiscip. Top.* **2001**, *64*, 020901.
(36) Dimova, R.; Pouligny, B.; Dietrich, C. *Biophys. J.* **2000**, *79*, 340−356.
(37) Steltenkamp, S.; Müller, M. M.; Deserno, M.; Hennesthal, C.; Steinem, C.; Janshoff, A. *Biophys. J.* **2006**, *91*, 217−226.
(38) Levien, R. *The elastica: a mathematical history*; UC Berkeley: Berkeley, CA, 2008; UCB/EECS-2008-103.
(39) Singer, D. A. *AIP Conf. Proc.* **2008**, *1002*, 3−32.
(40) Cooke, I. R.; Kremer, K.; Deserno, M. *Phys. Rev. E* **2005**, *72*, 011506.
(41) Cooke, I. R.; Deserno, M. *J. Chem. Phys.* **2005**, *123*, 224710.
(42) Marrink, S. J.; Risselada, H. J.; Yefimov, S.; Tieleman, D. P.; de Vries, A. H. *J. Phys. Chem. B* **2007**, *111*, 7812−7824.
(43) Limbach, H. J.; Arnold, A.; Mann, B. A.; Holm, C. *Comput. Phys. Commun.* **2006**, *174*, 704−727.
(44) Hess, B.; Kutzner, C.; van der Spoel, D.; Lindahl, E. *J. Chem. Theory Comput.* **2008**, *4*, 435−447.
(45) Michaud-Agrawal, N.; Denning, E. J.; Woolf, T. B.; Beckstein, O. *J. Comput. Chem.* **2011**, *32*, 2319−2327.
(46) Rosa, A.; Becker, N. B.; Everaers, R. *Biophys. J.* **2010**, *98*, 2410−2419.
(47) Bowick, M. J.; Sknepnek, R. *Soft Matter* **2013**, *9*, 8088−8095.
(48) Deserno, M. *Chem. Phys. Lipids* **2015**, *185*, 11−45.
(49) Oshri, O.; Diamant, H. From Compressible Elastica to Relativistic Dynamics and Back. 2015. arXiv:1506.07662. http://arxiv.org/abs/1506.07662, accessed Jun 2015.
(50) Landau, L. D.; Lifshitz, E. M. *Theory of Elasticity*; Butterworth-Heinemann: Oxford, 1999.
(51) Mills, J. K.; Needham, D. *Biochim. Biophys. Acta, Biomembr.* **2005**, *1716*, 77−96.
(52) Nagarajan, S.; Schuler, E. E.; Ma, K.; Kindt, J. T.; Dyer, R. B. *J. Phys. Chem. B* **2012**, *116*, 13749−13756.
(53) Needham, D.; Dewhirst, M. W. *Adv. Drug Delivery Rev.* **2001**, *53*, 285−305.

DOI: 10.1021/jacs.5b06800
J. Am. Chem. Soc. 2015, 137, 12752−12755